The International Journal of Cardiovascular Imaging (2019) 35:1483–1497
https://doi.org/10.1007/s10554-019-01603-y

ORIGINAL PAPER

Update on MR imaging of the pulmonary vasculature

Muhammad Aziz[1] · Mayil Krishnam[2] · Ananth J. Madhuranthakam[1] · Prabhakar Rajiah[1]

Received: 1 February 2019 / Accepted: 11 April 2019 / Published online: 27 April 2019

Abstract
Magnetic resonance imaging (MRI) plays an increasingly important role in the non-invasive evaluation of the pulmonary vasculature. MR angiographic (MRA) techniques provide morphological information, while MR perfusion techniques provide functional information of the pulmonary vasculature. Contrast-enhanced MRA can be performed at high spatial resolution using 3D T1-weighted spoiled gradient echo sequence or at high temporal resolution using time-resolved techniques. Non-contrast MRA can be performed using 3D steady state free precession, double inversion fast spin echo, time of flight or phase contrast sequences. MR perfusion can be done using dynamic contrast-enhanced technique or using non-contrast techniques such as arterial spin labelling and time-resolved imaging of lungs during free breathing with Fourier decomposition analysis. MRI is used in the evaluation of acute and chronic pulmonary embolism, pulmonary hypertension and other vascular abnormalities, congenital anomalies and neoplasms. In this article, we review the different MR techniques used in the evaluation of pulmonary vasculature and its clinical applications.

Keywords MR · MR angiography · MR perfusion · Pulmonary embolus

Pulmonary vasculature and its abnormalities can be evaluated using multiple imaging techniques, each with their own advantages and limitations (Table 1). Chest radiography provides an overview of the pulmonary vascular anatomy and secondary changes in lungs. It also distinguishes pulmonary hypertension (PHT) from shunt vasculature. Computed tomography (CT) is now the reference standard for the evaluation of pulmonary embolism (PE) [1]. It also provides information on the lungs as well as the heart which can be comprehensively evaluated using ECG-gating technique. CT is widely available and has a rapid turnaround time but involves the use of ionizing radiation and potentially nephrotoxic contrast media [2, 3]. Echocardiography is not adequate to evaluate pulmonary vasculature as such but is a widely available, cost efficient, non-radiation technique for the evaluation of the cardiac complications of pulmonary vascular abnormalities and also to screen for PHT. It is operator dependent and limited by acoustic windows, especially for the right heart structures. Nuclear medicine ventilation perfusion (V/Q) scan with or without SPECT was used commonly in the evaluation of acute PE, but currently used in this setting, only when CTPA is contraindicated or suboptimal. Scintigraphic lung perfusion scan is used in the evaluation of perfusion in chronic PE, PHT, shunts, congenital abnormalities and pre-surgical evaluation prior to lung surgery. Other limitations include the use of radiation, low spatial and temporal resolution, and soft tissue artifacts. 18F-FDG PET-CT can be used for evaluating pulmonary artery neoplasms or arteritis. Catheter pulmonary angiography provides high-resolution evaluation of the pulmonary vasculature, but because of its invasive nature, it is now reserved only for patients requiring interventional procedures. Right heart catheterization can also provide hemodynamic information, which is essential in PHT and other congenital abnormalities.

Magnetic resonance imaging (MRI) has now emerged as an important imaging technique for the evaluation of pulmonary vasculature, due to advances in scan technology and sequences. The advantages of MRI are its good spatial and temporal resolution that provides both anatomical and functional information, wide field-of-view and multi-planar acquisition/reconstruction capabilities that enables visualization of pulmonary as well as adjacent

✉ Prabhakar Rajiah
radpr73@gmail.com

[1] Department of Radiology, UT Southwestern Medical Center, Dallas, TX, USA

[2] Department of Radiology, University of California Irvine, Irvine, CA, USA

Table 1 Comparison of the different imaging modalities for evaluation of pulmonary vasculature

	Radiography	CT	Echocardiography	Nuclear medicine	MRI
Spatial Resolution	Inadequate	Excellent	Good	Average	Good
Temporal resolution	Not dynamic	Good	Excellent	Average	Good
Soft tissue contrast	Poor	Very good	Average	Poor	Excellent
Tissue characterization	None	Average	None	None	Excellent
Field-of-view	Limited	Excellent	Limited	Limited	Excellent
Evaluation of adjacent abnormalities	Average	Excellent	Average	Poor	Excellent
Radiation	Yes	Yes	No	Yes	No
Contrast nephrotoxicity	No	Yes	No	No	No
Optimal renal function	Not required	Required	Not required	Required	Controversial
Contrast allergy screening	Not required	Required	Not required	Required	Required
Screening for implants	Not required	Not required (May be evaluated for streak artifacts)	Not required	Not required	Required

structures, without the use of ionizing radiation or nephrotoxic contrast media. Spatial resolution of MRI is typically 1–2 mm, compared to 0.5 mm of CT angiography [4]. Tissue characterization is a major strength of MRI, due to the variety of MRI sequences that highlight different tissue properties, amplified with the use of intravenous gadolinium-based contrast agents. Cardiac sequela of pulmonary abnormalities can also be evaluated with dedicated cardiac MRI sequences. However, MRI cannot assess the lung parenchyma as good as CT and hence the pulmonary etiologies for pulmonary hypertension or sequela of pulmonary vascular abnormalities on lungs cannot be evaluated. MRI is also not as widely available as CT and requires advanced skills and expertise. Scan times can be long, which makes it inconvenient for patients who are unable to lay still for prolonged periods. MRI cannot be performed in patients with contraindications, including claustrophobia and several implanted metallic devices. However, MRI can now be safely performed in those with pacemakers/ICDs if appropriate precautions are taken [5]. Nephrogenic systemic fibrosis is a risk that has been reported in patients with severe renal dysfunction. Recent studies have shown that the incidence of this entity has decreased due to the establishment of safety procedures including the use of macrocyclic contrast agents. In the current practice, nephrogenic systemic fibrosis is essentially non-existent with the use of macrocyclic contrast agents. Gadolinium deposition in brain is another recent issue [6], seen in patients even with normal renal function parameters.

In the following sections, we review the MRI techniques used in pulmonary vasculature followed by the current role of MRI in the evaluation of various pulmonary vascular abnormalities.

MRI techniques in pulmonary vasculature

Morphological evaluation of the pulmonary vasculature, particularly the arteries and veins is performed using MR pulmonary angiography (MRPA), either with or without the use of gadolinium-based contrast. Functional evaluation of the pulmonary tissue perfusion at the capillary level is performed using MR perfusion techniques, which can also be performed with or without the use of intravenous contrast. Often, complementary information is generated by these two techniques (Table 2).

Contrast enhanced MRPA

Contrast enhanced MRPA provides high spatial resolution images of the pulmonary vasculature and is considered the most diagnostic of all the MR techniques [7]. Intravenous administration of a gadolinium-based contrast agent results in T1 shortening of adjacent tissues, which manifests as bright signal in MRA images (Fig. 1). Accurate timing is important to acquire the image when the contrast is present in the pulmonary vasculature, such that the center of k-space is filled at the same time using centric elliptic phase-encoding. This ensures high signal-to-noise ratio (SNR), and allows separation of arterial from venous phase. Typical injection protocols is 0.1 to 0.2 mmol/kg of gadolinium-based contrast, followed by a 20 ml saline bolus injected at 1–5 ml/s or 0.1 mmol/kg of contrast diluted with normal saline for a total volume of 30 mL, injected at 1.5 ml/s for a longer bolus [4, 8]. The optimal timing can be determined by tracking the bolus of contrast using a dynamic low resolution MR fluoroscopy and initiating acquisition when the contrast is just about to enter

Table 2 Summary of MR techniques used in pulmonary vasculature

MR Angiography		MR Perfusion	
Contrast	Non contrast	Contrast	Non Contrast
3d T1-w spoiled gradient echo	3d- balanced steady state free precession	3d T1-w spoiled gradient echo	Fourier decomposition with cyclic lung signal intensity differences with image subtraction
Time Resolved MRA (TRICKS, TWIST)	Fresh blood imaging using 3d partial Fourier Fast Spin Echo (FSE)	Time Resolved MRA (TRICKS, TWIST)	ASL, pASL, CASL
Blood pool contrast imaging	Arterial spin labelling (ASL)		SEEPAGE
	Time of flight		
	Phase contrast		

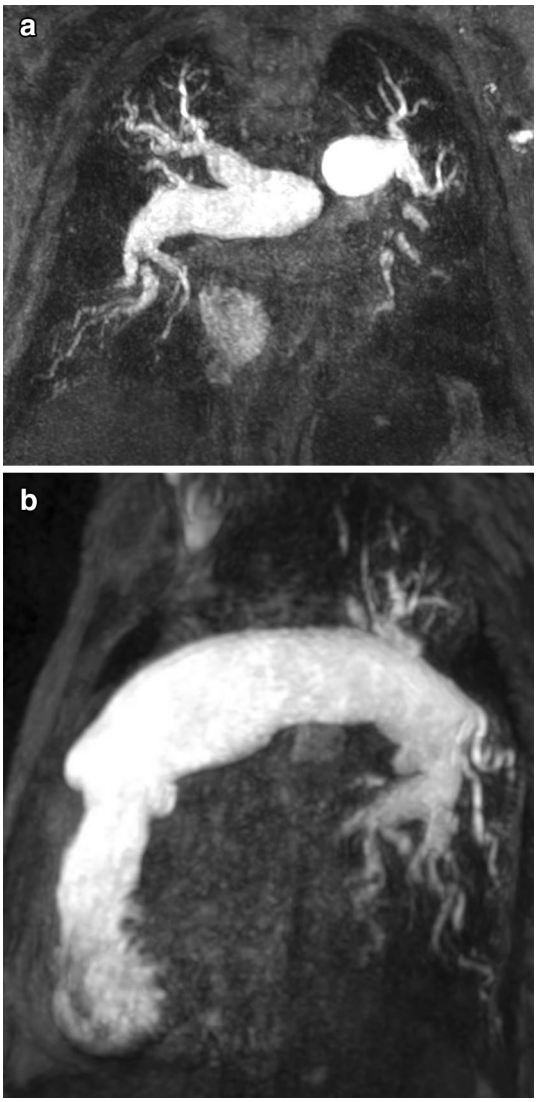

Fig. 1 MR pulmonary angiography- MR pulmonary angiography in 61-year-old man with pulmonary hypertension in the coronal (**a**) and sagittal (**b**) planes show markedly dilated pulmonary arteries

the pulmonary arterial tree. Alternatively, the optimal timing can be determined with the use of a test bolus injection using 1–2 ml of the contrast agent to measure the arrival time of the contrast to the desired vasculature. Usually the scan is performed over two breath-holds, with two phases of acquisition at each breath hold. 3D T1-weighted spoiled gradient echo sequence is utilized with typical acquisition values of: TR = 2.5–3 ms, TE = 1.0–1.5 ms, Flip angle = 30–40°, matrix = 40 × 192 × 256, FOV = 460 mm and parallel imaging factor (R) of 2 [8]. Isotropic spatial resolution can be obtained by acquiring data in an oval area of k-space (Elliptic phase encoding) and zero-filling the corners [4]. TE and TR can be reduced by fractional echo read-out. Spatial resolution of 2 mm in phase encoded direction and 1.5 mm in frequency encoded direction can be achieved [4].

Time resolved magnetic resonance angiography (TR-MRA) sequences like TWIST—*time-resolved imaging with stochastic trajectories* (Siemens Healthcare, Erlangen, Deutschland), or TRICKS—*time-resolved imaging of contrast kinetics* (General Electric Healthcare, Milwaukee, WI, USA) enable dynamic acquisitions and improved temporal resolution (up to 1 second) without sacrificing spatial resolution. These techniques operate by more frequent sampling of the center of the k-space than the peripheral sections of a 3D acquisition to generate multiple images after the administration of the contrast agent [9, 10]. Missing data at each time point are shared between k-spaces using several methods including keyhole imaging, view sharing, under-sampled projection reconstruction [11], zero filling [12] and spiral TRICKS acquisitions [13], without significant loss of spatial resolution. Power injector-based contrast administration has been shown to be associated with a more standardized scan protocol compared to manual injection [14].

Blood pool, intravascular contrast agents stay for prolonged periods in the blood due to their high molecular weight and albumin binding. Typical agents include Gadofosveset trisodium (Ablavar), and Gadomer-17.

Ferumyoxtol, is an ultra-small superparamagnetic iron oxide (USPIO) particle [15] that can be used in patients with contraindication to Gadolinium-agents. The larger size of the molecule minimizes extravascular leakage and carbohydrate coating prevents glomerular filtration [15]. These facilitates the use of low contrast dose and multiple repeat image acquisitions without worrying about contrast leaving the vasculature of interest [16]. It is particularly useful in patients who cannot hold their breath. Higher spatial resolution and even ECG-gating can be performed. Although this results in ability to image without strict time windows, arterial and venous phase separation is compromised.

3D radial ultrashort echo time (UTE) sequence has been used in dogs to obtain high resolution images of morphology and perfusion [17].

Non-contrast MRPA

Non-contrast MRA is useful in patients with severe renal dysfunction, who are not suitable for getting intravenous contrast media [18]. It is also useful in pregnant women, who cannot have gadolinium-based contrast. 3D-Balanced steady state free precession (bSSFP) sequence is a commonly used sequence, that achieves T2/T1 weighting by frequent radiofrequency (RF) pulse phase alteration, and gradient echo refocusing resulting in a steady state. Blood appears bright due to long T2 with a high signal contrast to surrounding tissues and can provide an effective detection of thrombus and other lesions. bSSFP sequences are sensitive to field inhomogeneities and a very short TR (e.g. 2–3 ms) is required to minimize the artifacts [19].

Fresh blood imaging technique uses ECG-gated 3D partial Fourier Fast spin echo (FSE) technique. With this sequence, arterial blood appears dark in systole due to flow void and high in diastole due to comparatively slow flow. Veins show some signal both in systole and diastole due to slower flow rate. Subtraction of the systolic and diastolic images will thus produce an image with bright signal in the arteries and no signal in the veins [20]. This technique is prone to misregistration, and not routinely used in the diagnosis of PE. Traditional FSE imaging with double inversion (DI-FSE) also shows blood as dark, and hyperintense appearance in slow flow or presence of thrombus.

Arterial spin labelling (ASL) is a non-contrast imaging technique that uses slice selective acquisition with repeat imaging after initial inversion pulse. It can be useful in combination with faster acquisitions like partial-Fourier single-shot FSE and bSSFP. ASL acquires two images—one where the upstream blood is 'tagged' with an inversion RF pulse, and the other image without any blood "tagging. The subtraction between the two images generates signal only from the "tagged" blood, that can be used to visualize vasculature and tissue perfusion [20].

Routine non contrast MRA techniques like phase contrast and time of flight (TOF) imaging are of equivocal usefulness in the chest, although there have been reports of 3D and 4D TOF imaging. TOF technique is based on a gradient echo (GRE) acquisition depending on the movement of protons. With TOF, the stationary tissues within the imaging FOV are saturated by the repeated RF excitation pulses, while the fresh flowing blood from the outside of the imaging FOV retains higher signal. Thrombosis can be seen as a filling defect or a low intensity focus. Phase contrast imaging is another gradient echo based acquisition, where the phase accumulation due to the flowing blood are converted into signal intensity causing thrombosed area to appear with higher signal intensity. Both TOF and phase-contrast methods require longer acquisition times and are limited due to the cardiac and respiratory motions.

Contrast enhanced MR pulmonary perfusion

Contrast-enhanced MR perfusion is typically obtained by dynamic time-resolved MRA sequence and subtracting peak first-pass dynamic post-contrast T1-weighted images from a pre-contrast acquisition. A lower quantity of gadolinium can be used than a full contrast enhanced MRPA, i.e 0.05 ml/kg. Perfusion imaging typically has lower spatial and higher temporal resolution than a conventional MRPA, and is acquired with long breath-hold or shallow free breathing. A 3D GRE sequence at 5–10 mm slice thickness typically results in a temporal resolution of 1.0–1.5 s [21]. Temporal resolution can be increased by parallel imaging and view-sharing. The spatial resolution can be increased by judicious use of parallel imaging. Typical imaging parameters are: TE = 0.8–1.0 ms; TR = 2.0–2.5 ms, $\alpha = 30–40°$, FOV: 460 mm, and matrix: $32 \times 96 \times 128$ [8]. Perfusion abnormalities can be qualitatively assessed, typically seen as wedge shaped segmental or sub-segmental defects in acute PE, wedge shaped or mottled defects in CTEPH and diffuse defects in PHT [7]. Quantitative metrics can be obtained following image reformatting and post-processing including pulmonary blood volume (PBV), pulmonary blood flow (PBF), mean transit time (MTT) and time to peak (TTP). MTT is calculated as PBV/PBF, typically increased in PHT and CTEPH and may decrease following successful treatment [7]. Suspected vasoconstriction due to hypoxia in COPD results in decreased MTT, PBF and PBV [7]. For absolute quantification, measurement from a central pulmonary artery or right ventricle is used to obtain arterial input function (AIF). Signal intensity over time is converted to contrast concentration. Dual-bolus approach with higher volume bolus following initial low volume enables a linear signal and contrast concentration relationship which permits higher lung perfusion quantification.

3D time-resolved sequences like TRICKS or TWIST with dynamic imaging are also helpful in identification of cardiac shunts and perfusion defects in a regional distribution. These are vulnerable to temporal interpolation artefact and thus need to be used with care.

Non-contrast MR pulmonary perfusion

Non-contrast pulmonary perfusion can be obtained using Fourier decomposition with imaging of cyclic lung signal intensity differences with image subtraction [22] during breathing and cardiac rhythms. With inspiration, the lung signal decreases and with expiration it increases. In systole, signal is low due to high velocity and the signal is high in diastole. Perfusion-weighted images may be obtained due to the different frequencies.

Arterial spin labeling (ASL), as described above, also results in useful perfusion imaging of the pulmonary vasculature. Signal proportional to the pulmonary artery flow is obtained on the perfusion weighted image after subtraction of tagged image from source image. Multiple newer sequences result in improved labelling including pulsed ASL, pseudo-continuous ASL (pASL) or continuous ASL (CASL) (Fig. 2). Few pulsed ASL sequences like Flow sensitive alternate inversion recovery with extra radio frequency pulse (FAIRER) and Flow sensitive alternative inversion recovery (FAIR) can help quantify regional perfusion by subtraction of a nonselective inversion pulse from a selectively inverted image, with the difference proportional to the perfusion [23]. ASL done at 3 T reduces imaging time to 6–8 min with FAIR sequence [24].

Other newer sequences utilizing single shot sequences with signal acquired only from the previously "tagged" blood with suppression of background soft tissue, termed SEEPAGE (spin echo entrapped perfusion image) [25] avoid the need for registration. Background suppression can also help remove background signal inhomogeneity and motion artifacts [24]. Higher field strength can provide higher signal to noise ratio (SNR) however susceptibility effects due to increased B0 inhomogeneities are also increased.

Non-contrast MR perfusion is still in early stages of clinical use due to known limitations including longer acquisition time, comparatively lower resolution and low SNR. It is of most use in patients with renal failure and especially those with need for repeated scans without concern for renal clearance of contrast.

Supplemental imaging of the heart and lungs

MRI also allows the evaluation of lungs and the heart. Lungs can be evaluated using single-shot fast spin echo (RARE/HASTE, Turbo FSE). Cine b-SSFP sequence also provides morphological and functional information of the heart. Velocity encoded phase contrast (VE- PC MRI) sequence is used for providing hemodynamic information, including the flow, velocity and pressure gradients. Late gadolinium

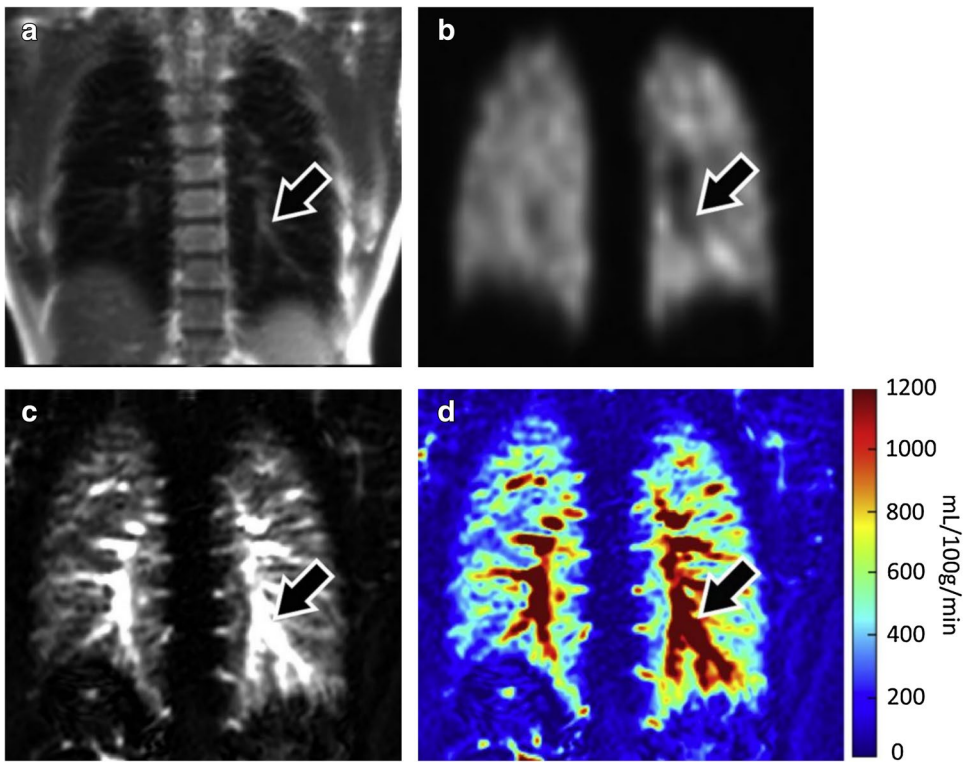

Fig. 2 MR perfusion- Coronal proton density weighted image (**a**), SPECT perfusion image (**b**), FAIR perfusion-weighted image (**c**), and reconstructed perfusion map derived from FAIR perfusion (**d**) in a 33-year old healthy female volunteer. Arrows indicate signals from major vessels that are visible on FAIR perfusion images (**c**, **d**), and seen as regions of photopenia on SPECT images (**b**). Reproduced from Greer et al (22), with permission from Elsevier

enhancement sequences are used for identifying and quantifying myocardial scarring or fibrosis. Parametric mapping techniques such as T1 and T2 provide quantitative imaging biomarkers, that can identify myocardial changes at an earlier stage, such as diffuse fibrosis [26].

Clinical applications of MRI in pulmonary vasculature

MR angiography and perfusion techniques are used in the evaluation of several disorders of the pulmonary vasculature, which are described in detail in the following sections.

Acute pulmonary embolism

Acute pulmonary embolism (PE) is a potentially life threatening condition, that is typically caused by lower extremity thrombus. CTPA is the current standard of care due to high accuracy, wide availability and rapid turnaround time as well as the ability to evaluate for other causes of chest pain [27, 28]. The use of MRA has traditionally been lower in acute PE due to lack of familiarity, need for higher expertise, longer scan time, limited availability, limited volumetric coverage, lower spatial resolution and artifacts [4]. MRI acquisition time has come down due to advances such as parallel imaging, view-sharing and time-resolved MRA [29]. MRA is a viable alternative to CTPA that provides comparable information without radiation dose, particularly valuable in younger patients.

An abbreviated MRPA protocol has been described for acute PE, which typically takes six breath holds (end-expiration), totally lasting 10 min. This includes—three-plane single-shot fast spin echo localizers; pre-contrast T1-weighted 3D spoiled gradient-echo (SGRE); pulmonary arterial phase 3D T1-W SGRE; Immediate post-contrast T1-W 3D SGRE; Post-contrast low flip-T1-w 3D SGRE at low flip angle (15° versus 28°); and T1-w 3D SGRE with fat saturation [4]. The arterial phase is timed using fluoroscopic triggering and obtained using elliptical centric k-space filling. The lower flip-angle approximates the optimal flip angle for blood. Fat saturation sequence is useful for enhancing soft tissue abnormalities. Slab excitation is performed in the sagittal plane and 2D parallel imaging in both phase-encoding directions, with net acceleration of 3.7 is used [4]. Use of 2D parallel imaging helps in improving spatial resolution with shorter acquisition time [29]. A second injection can be administered in suboptimal studies.

MRA findings of acute PE include occlusive or non-occlusive filling defect in the pulmonary arteries (Fig. 3), which makes an acute angle with the vessel wall and expands the lumen. Occlusive emboli are often seen as abrupt vessel cut-offs, which may be more challenging than CTA to identify [4]. Perfusion can be evaluated in the arterial phase MRA sequence or a dedicated time-resolved perfusion scan acquired prior to pulmonary MRA [4]. Wedge shaped segmental or sub-segmental perfusion defect in the lungs, which show a good inter modality agreement with SPECT [30]. While scintigraphy involves deposition of radio-isotopic particles in small capillaries and arterioles of the lung, MR is dynamic first-pass acquisition during contrast, typically every 0.5 s [31]. In severe PE, secondary changes can be seen in the heart including dilated RV, RV dysfunction, tricuspid regurgitation, and reflux of contrast into the IVC and hepatic veins. Incidental findings can be evaluated in the localizers and post-contrast scans.

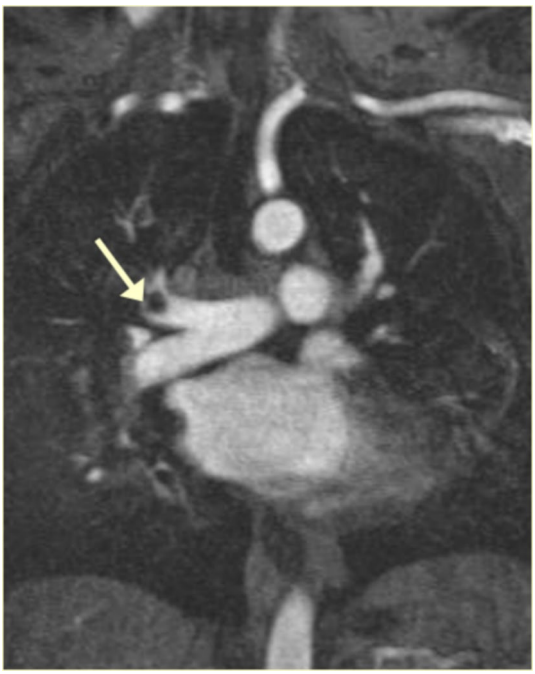

Fig. 3 Acute pulmonary embolism—Coronal MR angiographic image shows a central filling defect in a right upper lobar artery (arrow), consistent with an acute pulmonary embolism

Prospective investigation of pulmonary embolism diagnosis III (PIOPED III) study which had various tests as reference standard found that with technically adequate scans, the sensitivity of MRPA was 78% and specificity was 99% [32]. The negative predictive value for exclusion of PE is > 97%. However, there were a significant number of inadequate scans, with a mean of 25% and range of 11–52%, mostly due to poor contrast or motion [32]. If technically inadequate scans were included, PE was diagnosed in only 57% of all patients with known PE [32]. Combined MR PA and MR venography had sensitivity of 92% and specificity of 98%, but 52% of patients had technically inadequate scans [32]. Hence, the authors recommend the use of MRPA only in patients with contraindications to other modalities,

and in centers which have more advanced MRPA programs [32]. It should be noted that in this study, only a single MR sequence (3D CE-MRA) was utilized and multiple different MRI systems were utilized as part of a multi-center study.

The performance of MRI has been shown to be improved since the PIOPED III study, advances in MRI hardware and software, including 2D parallel imaging, diluted contrast bolus and multiple acquisitions. Using these techniques, one study showed that 60% of examinations were considered to be in the best category, compared to 26% in PIOPED study [4] One study from Europe using multiple MR sequences showed high sensitivity for central pulmonary arteries of 98–100% [33]. Schiebler et al. showed that the negative predictive value of MRPA was comparable to CTPA, with 97% NPV at 3 months, and 96% NPV at 1 year follow up [34]. This establishes the usefulness of pulmonary MRA as a first line diagnostic tool. Another study showed high performance of MRPA in diagnosis of PE in central and segmental branches with sensitivity of up to 84% and specificity of 100% [35]. MRA may not be good for subsegmental PE, but these are not generally considered significant. Artifacts include truncation, which produces signal drop in the center, which is typically less than 50% [4, 36]. Early acquisition of contrast may result in enhanced edges, whereas late acquisition results in blurry edges [4]. Motion artifacts are most likely in the pulmonary arterial phase. Perfusion abnormalities can also be seen in lung parenchymal abnormalities. A real-time cine SSFP image has also been used as a non-contrast MRA technique useful in pregnant patients. This has a 83% sensitivity and 100% specificity compared to scintigraphy and 93% sensitivity and 100% specificity compared to contrast-MRA [37].

MR can be used to evaluate the extent of disease and predict outcome in patients with PE. In a small study with 50 patients, PBF derived from perfusion MRI was significantly more accurate parameter than RV/LV diameter ratio, CT index and MRIA index. The specificity and accuracy of perfusion MRI and RV/LV diameter were significantly higher than CT and MRA PE indices [38].

Chronic pulmonary embolism

Acute PE can evolve to chronic PE in a small subset and then result in chronic thromboembolic pulmonary hypertension (CTEPH) in a smaller subset of patients, i.e 0.5 to 3.8% [39]. CTEPH is diagnosed when there is pulmonary hypertension and persistent perfusion defect. CTEPH is potentially curable, and hence needs to be recognized. MRPA shows vascular morphological changes of chronic PE similar to CTPA, including vessel wall thickening, organized thromboemboli, irregularity, vessel cut-offs and intraluminal webs & bands [40] (Fig. 4a). MR also shows features of PHT as elaborated in the paragraph below. MRI is also superior to

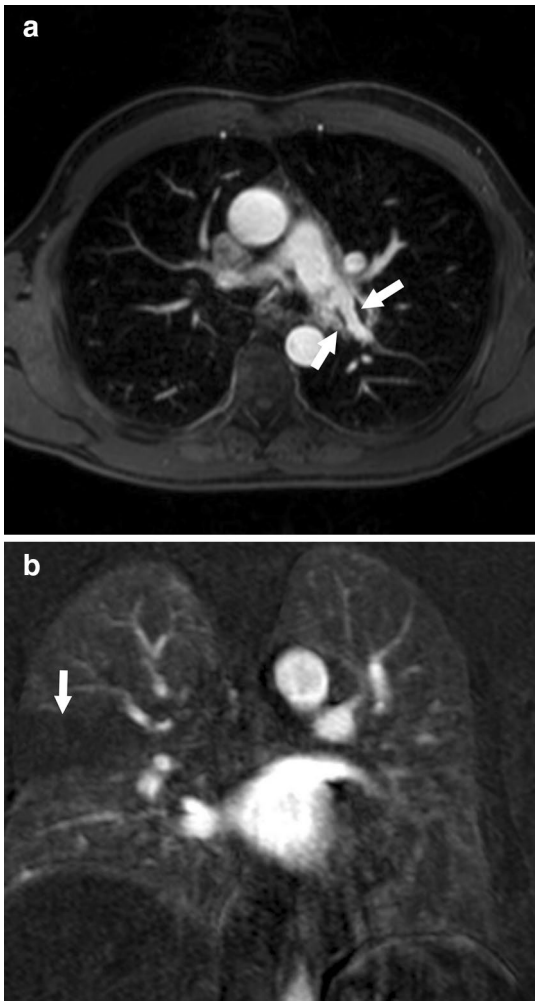

Fig. 4 Chronic pulmonary embolism: **a** axial MR pulmonary angiogram shows eccentric filling defect in the left main pulmonary artery with obtuse angles with the lumen consistent with chronic pulmonary embolism (arrow), **b** coronal MR angiographic image in another patient shows a wedge shaped filling defect (arrow) in the right upper lobe, from a previous episode of pulmonary embolism

digital subtraction angiography (DSA), with sensitivity and specificity of MRI for main/lobar and segmental levels of 83.1%/98.6% and 87.7%/98.1% compared to 65.7%/100% and 75.8%/100% for DSA [41]. Another study showed that MRI depicted pulmonary vessels up to segmental level in all cases, whereas for subsegmental arteries, DSA revealed more patent vessel segments than MRA [42]. Another study showed that CE-MRA has a overall sensitivity and specificity of 98% and 94% respectively in diagnosing CTE. The sensitivity of central vessel disease improved from 50 to 88% when CE-MRA was analyzed along with unenhanced proton MRA with SSFP, which delineates the vessel wall better [43].

Perfusion defects are seen in chronic PE, which are comparable to perfusion scintigraphy [44] (Fig. 4b). Perfusion

defects are also seen in CTEPH, which are more focal compared to diffuse distribution in idiopathic pulmonary arterial hypertension (IPAH) [45]. Although, perfusion defect identified in ventilation/perfusion (V/Q) scintigraphy is routinely used for the diagnosis of CTEPH, this is associated with the use of radiation. MR perfusion has a sensitivity of 97% and specificity of 92% compared to perfusion scintigraphy, making it an attractive initial imaging modality without the use of radiation [44]. A recent study found that MRI perfusion is in fact superior to SPECT V/Q scintigraphy, with 100% sensitivity of MRI compared to 97% for SPECT perfusion, making MRI an ideal first line screening tool without the use of ionizing radiation [31]. This higher sensitivity of MRI in chronic PE than acute PE, could be because CTPA can detect even small clots in the acute setting, which are beyond the resolution of MRI. However, these smaller peripheral PE are unlikely to cause CTEPH and hence MRI is unlikely to miss the emboli causing CTEPH [31]. Another study showed that CT and MRI are complementary modalities, with CT being good for parenchymal and vascular abnormalities, MRI is good for lung perfusion and right heart function [39].

Reduced pulmonary blood flow (PBF), mean transit time (MTT), and pulmonary blood volume (PBV) can be seen. Significantly improved pulmonary blood flow, mean pulmonary arterial pressure and clinical performance were noted postsurgical treatment (endarterectomy) on a recent study [46]. The PBF improvement was predominantly in the lower lungs, with the magnitude of improvement of PBF improvement in lower lobes correlating with improvement in exercise capacity [46]. Another study showed there was decreased RV ejection fraction and pulmonary peak velocity in CTEPH patients before surgery. Following surgery, there was improvement of RV ejection fraction (that correlated with PVR and mPAP) and peak pulmonary velocity [42].

Pulmonary hypertension

MRI is an ideal technique for the evaluation of PHT. The various uses of MRI in this clinical setting include- establishing etiology, non-invasive hemodynamics, quantification, prognosis, risk stratification and monitoring response to therapy. Typical PHT findings are well visualized on MRA including dilated central pulmonary arteries (Fig. 5a), with the main pulmonary artery diameter (MPA) > 2.9 cm and ration of MPA to ascending aorta of > 1. On dark blood images, higher signal intensity in the MPA indicates mean arterial pressure of > 70 mm Hg and higher pulmonary vascular resistance (Fig. 5b) [47, 48]. Lower velocity and retrograde flow in MPA in phase contrast imaging is also indicative of PHT very high sensitivity of more than 92% [49].

Ley et al. showed that increased MTT is the only measurable effect of PHT on pulmonary perfusion [50]. There was only moderate linear correlation with mPAP [50]. Another study showed linear relationship was demonstrated between PBF and mPAP as well as between PBV and mPAP [51]. This can be potentially used to monitor therapy and also to understand the pathophysiology. Pulmonary transit time in CE-MRA was prolonged in patients with PHT, and this correlated with pulmonary vascular resistance, right ventricular stroke volume index and pulmonary capacitance [52]. Another study showed that higher pulmonary transit time and full-width half maximum of the first pass clearance curve with dynamic contrast enhanced MRI were associated with poor outcome and were strong predictors of adverse outcome [53]. Average pulmonary artery blood velocity throughout the cardiac cycle strongly correlates with pulmonary pressures and resistance [49]. They are associated with clinical gold standards of pulmonary vascular resistance index and cardiac index. Using 4D flow MRI, the duration of vorticeal blood flow in the main pulmonary artery was increased, with presence ≥ 14.3% of the entire cardiac cycle correlating with high mPAP and indicative of PH, with high 97% sensitivity and 96% specificity [54]. One study showed that in patients with idiopathic PHT and CTEPH, increases in MRI pulmonary perfusion and mean MR flow peak velocity were seen after 3 weeks of physical training, along with improved 6 min walking distance [55].

Cardiac findings secondary to PHT include increased right heart chamber volumes and hypertrophy (Fig. 5c), systolic interventricular septal flattening or bowing towards the LV (Fig. 5d) and wall motion abnormalities. Late gadolinium enhancement may be seen at RV insertion points (Fig. 5e), due to pressure overload and correlates with features such as RV mass, volume and dysfunction. MRI provides a one-stop shop evaluation of the morphology, perfusion and secondary effects on the heart.

Other pulmonary vascular abnormalities

MRI is an ideal imaging technique in the evaluation of other pulmonary vascular abnormalities. Pulmonary artery stenosis (narrowing) can be seen due to chronic PE or trauma as well as extrinsic compression by masses such as bronchogenic carcinoma and fibrosing mediastinitis. On SSFP images, a jet of high velocity can be seen. The velocities and pressure gradients can be quantified using phase-contrast MRI. True aneurysm of the pulmonary artery (Fig. 6) can be seen in PHT, chronic PE, vasculopathy, vasculitis, iatrogenic, trauma, infection and neoplasm [56].Congenital deficiency of the wall and pulmonic stenosis are also causes of aneurysms. Pseudoaneurysm does not have all the three layers and is usually caused by iatrogenic or traumatic injuries, or infections. Idiopathic pulmonary arterial dilation is diagnosed when there is no other etiology to account for the dilation. Pulmonary artery is involved in several arteritis, particularly Takayasu, Behcet's syndrome and Hughes-Stovin

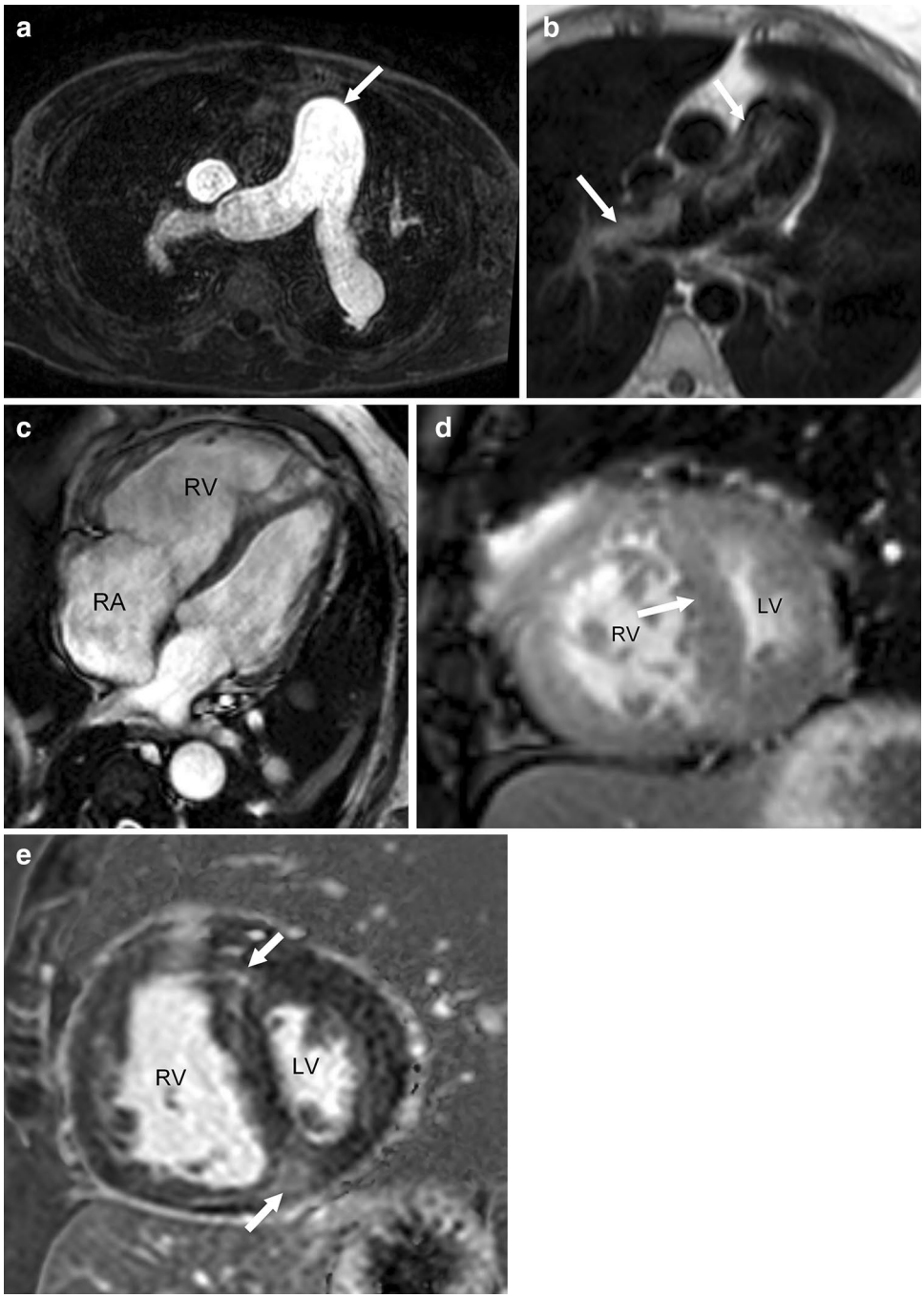

Fig. 5 Pulmonary hypertension: **a** Axial MRA image shows dilated central pulmonary arteries, **b**. Axial black blood double inversion recovery MR Image shows signal within the central pulmonary arteries due to slow flow, which is a feature of pulmonary hypertension, **c** 4-chamber cine SSFP image shows dilated and hypertrophied right ventricle, dilated right atrium and flattening of the ventricular septum, which are sequela of pulmonary hypertension, **d** short axis cine SSFP MR image shows severe hypertrophy of the right ventricle and systolic bowing of the ventricular septum towards the LV due to pressure overload, **e** short axis inversion recovery image obtained 10 min after contrast administration shows abnormal late gadolinium enhancement in the septum at sites of RV insertion (arrows), due to pressure overload

syndrome. MRA demonstrates stenosis and aneurysms which are sequela of arteritis. MRI can also image the arterial wall and estimate the activity of the disease. Presence of wall thickening is seen in both active and inactive disease, but wall edema (seen in T2—fat suppressed images) and delayed contrast enhancement are seen only in active stages (Fig. 7). Hughes–Stovin syndrome has thrombophlebitis and rupture in addition to pulmonary artery aneurysms. Behcet's syndrome has aneurysm, thrombosis, pulmonary infarction, hemorrhage and pleural effusion [56].

Congenital anomalies

MRA is used in the evaluation of severe congenital pulmonary vascular abnormalities, including pulmonary to systemic shunts, pulmonary atresia, pulmonary sling, anomalous pulmonary and coronary artery origin, anomalous pulmonary venous return, patent ductus arteriosus and arterio-venous malformations. Congenital causes of pulmonary stenosis include Tetralogy of Fallot, and syndromes such as Williams, Ehler-Danlos and Downs. Pulmonary stenosis is

Fig. 6 Pulmonary artery aneurysm—Sagittal SSFP image through the heart shows an aneurysmal dilation of the main pulmonary artery (arrow). There is mild compression of the left anterior descending artery (arrowhead)

also seen as a complication of congenital heart disorders, including Tetralogy of Fallot and transposition of great arteries (Fig. 8). Pulmonary atresia shows abrupt termination of the main pulmonary artery after its origin. Collateral vessels may be seen, particularly major aortopulmonary collaterals. Pulmonary sling shows origin of left pulmonary artery from the right pulmonary artery and running between esophagus and trachea. MRPA techniques have shown to be highly useful in the identification of intrapulmonary shunt volumes. Pulmonary artery and aortic flow measurements help determine left to right shunting with cine sequences useful in assessment of cardiac septal defects [57]. Pulmonary arteriovenous malformations were assessed on one study [58], with evaluation of pre and post-embolization reperfusion by another team [59].

Parenchymal and acquired abnormalities

Additional applications of MR perfusion include assessment in cystic fibrosis patients often providing a more sensitive assessment of parenchymal changes compared to CT scan, providing a biomarker that is used in evaluation of disease progression and in assessment of post treatment changes [60]. In addition to perfusion defects, parenchymal changes are also seen on MRI including bronchial wall thickening, bronchiectasis and mucoid impaction. The diagnostic utility of MR perfusion was shown to be comparable to dynamic contrast enhanced MRI with non-contrast Fourier decomposition (FD) magnetic resonance (MR) imaging [61].

MR perfusion is also of use in chronic obstructive airway disease (COPD), where perfusion defects are not typically

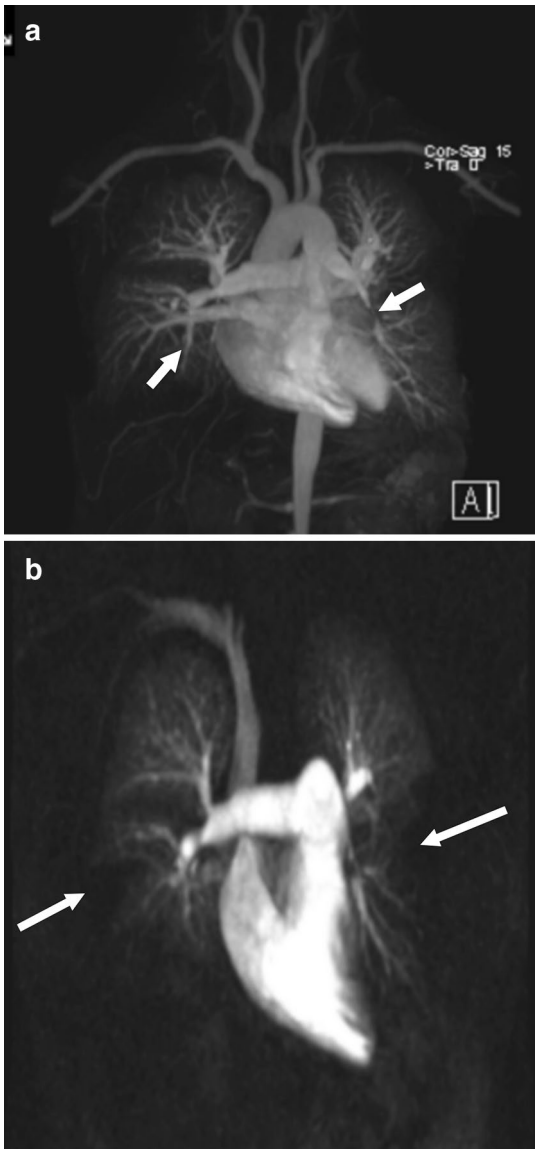

Fig. 7 Arteritis. 30-year-old female with large vessel vasculitis: **a** high spatial resolution MR angiographic image shows narrowing of bilateral lower lobar pulmonary arteries (arrows), **b** time-resolved MR angiography in the same patient shows perfusion defects (arrows) in both the lungs

wedge shaped as opposed to vascular etiologies like PE [30]. Quantitative MR perfusion, such as positive enhancement integral have been shown to be capable of distinguishing smokers with normal lung from mild COPD, with higher sensitivity than CT [62]. Heterogeneously reduced kinetics including PBV, PBF and MTT [63] are also noted in COPD, likely secondary to hypoxia due to vasoconstriction. Inverse relation is seen between MR perfusion and COPD severity and/or emphysema, with low PBF and PBV seen in such patients with worse airflow limitation on PFT and emphysema index on CT [64]. There is also absence of

Fig. 8 Pulmonary stenosis. Contrast enhanced MR angiography shows stenosis of the left pulmonary artery (arrow) in a patient following arterial switch repair for D-Transposition of great arteries. Note the draping of the pulmonary arteries over the ascending aorta, which is a normal appearance in this surgery due to LeCompete maneuver

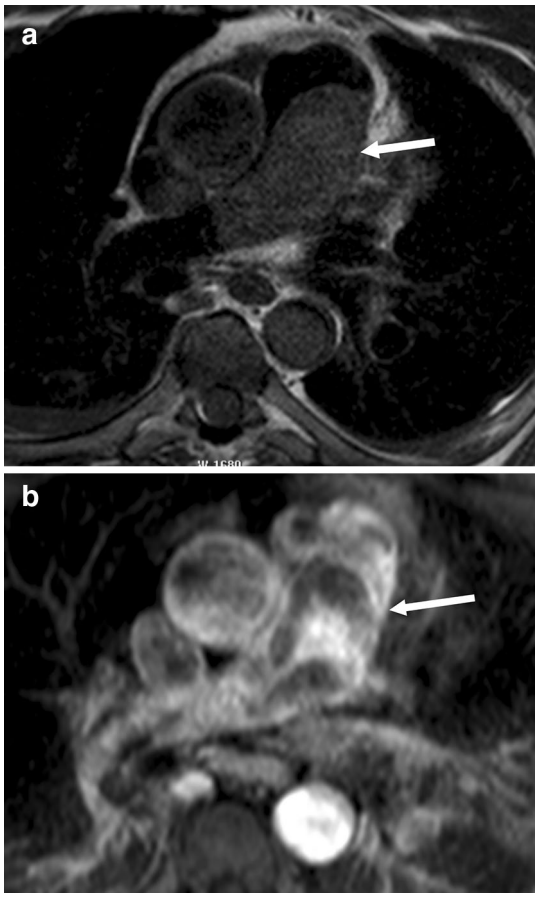

Fig. 9 Neoplasm. **a** Axial pre-contrast T1-weighed image shows a large hypontense mass (arrow) in the main pulmonary artery that expands the artery, **b** contrast- enhanced T1-weighted image shows intense heterogeneous enhancement of the mass (arrow), which is consistent with a sarcoma

normal expected increase in PBV with expiration [65]. In acute exacerbation of COPD, reduction of PBF and PBV and significant prolongation of MTT and TTP were noted, with increased PBV and PBF and decreased MTT and TTP noted with stabilization [66] One study interestingly looked at MR perfusion in smokers demonstrating varying degree of reduced perfusion and showed more abnormalities than corresponding CT scans [67]. MR pulmonary perfusion can help differentiate between different phenotypes of COPD with small perfusion defects in mild emphysema with bronchial wall thickening; and middle sized perfusion defects in emphysema with bronchial wall thickening [68].

Using multiphase dynamic enhancement and T2-weighted triple inversion recovery black blood TSE images on 3 T, inflammatory lesions of lung fibrosis showed early enhancement, whereas fibrosis-predominant biopsy sites showed late enhancement [69]. MRPA has also shown to be of some value in the evaluation of solitary pulmonary nodules [70]. This study by Ohno et al. showed higher usefulness of CT dynamic first pass contrast perfusion compared to dynamic first pass contrast MRI with very short TE [70].

Neoplasms

Neoplasms are rare in the pulmonary arteries, and can be either benign or malignant. Bronchogenic neoplasm is the most common malignancy to involve the pulmonary artery. Sarcoma can be occasionally seen in pulmonary arteries, originating in the sub-intimal and intimal layers. Intimal lesions grow inside the artery, and can be confused with PE, but heterogeneous contrast enhancement, and expansion of the arterial lumen favor the diagnosis of malignancy (Fig. 9).Pre surgical pulmonary MRA assessment in patients with lung cancer can be used using both contrast enhanced and non-contrast MRA equally well [71]. Non contrast pulmonary MR perfusion has also been shown to be of value in predicting lung function post lung cancer resection equivalent to a multi-detector CT scan and contrast enhanced perfusion MR [72] and better than perfusion scan. Better anatomic and postoperative lung functional assessment was also seen compared to perfusion scans. Dynamic first pass MR perfusion has been evaluated in diagnosis of solitary pulmonary nodules, however were found inferior to dynamic first pass contrast enhanced perfusion area detector CT [70] as detailed above.

Venous disorders

MRA is also useful in the evaluation of pulmonary venous abnormalities. Stenosis of the pulmonary vein has been evaluated with pulmonary MRA, with corresponding reduced flow in ipsilateral lung [73]. Pulmonary vein anatomy is also evaluated prior to radiofrequency ablation for atrial fibrillation using MRI. Variations including accessory ostium and common ostium are evaluated. Pulmonary veins can be measured to accurately size the catheters and also evaluate for pulmonary stenosis. Anomalous pulmonary venous return with one of the branches of the pulmonary vein on either or both sides not draining into the left atrium (Fig. 10), and may be seen draining into superior or inferior vena cava, pulmonary arteries or another systemic vessel. An anomalous venous return of the entire lung, usually on the right, associated with hypoplasia of the right lung and pulmonary artery is a characteristic feature of Scimitar syndrome (Fig. 11). The anomalous vein usually drains inferiorly into the IVC, coursing through the diaphragm. Postoperative anatomy in complex postsurgical congenital cardiac cases also often involve pulmonary vasculature and may be assessed accurately with pulmonary MRA.

Conclusion

MRA of the pulmonary vasculature and MR perfusion of the lungs can be performed either with or without intravenous contrast. MRA is now used in the evaluation of pulmonary embolism, pulmonary hypertension, congenital anomalies, neoplasms and venous anomalies. MR perfusion techniques have been shown to be most useful in the evaluation of chronic thromboembolic pulmonary hypertension.

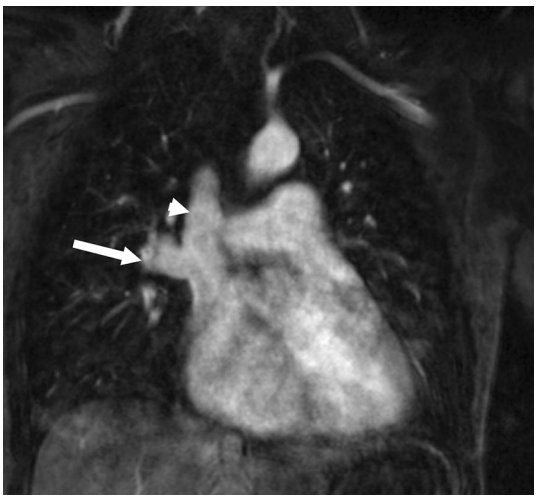

Fig. 10 Partial anomalous pulmonary venous drainage. Coronal MIP image from MRA shows a partial anomalous vein of the right upper lobe (arrow) which is draining into the superior venacava (arrowhead)

Fig. 11 Scimitar syndrome. High resolution MR Angiogram shows an anomalous pulmonary vein (arrow) supplying the right lower lobe and draining into the inferior venacava (arrowhead). Note that the right lung is smaller than the left, which is a feature of this syndrome

Funding The paper did not receive any external or internal funding.

Compliance with ethical standards

Conflict of interest There is no conflict of interest and no financial disclosure.

Ethical approval This study did not involve research involving human participants and/or animals and did not require informed consent.

References

1. Moore AJE, Wachsmann J, Chamarthy MR, Panjikaran L, Tanabe Y, Rajiah P (2018) Imaging of acute pulmonary embolism: an update. Cardiovasc diagn ther 8(3):225–243. https://doi.org/10.21037/cdt.2017.12.01
2. McDonald RJ, McDonald JS, Bida JP, Carter RE, Fleming CJ, Misra S, Williamson EE, Kallmes DF (2013) Intravenous contrast material-induced nephropathy: causal or coincident phenomenon? Radiology 267(1):106–118. https://doi.org/10.1148/radiol.12121823
3. Wilhelm-Leen E, Montez-Rath ME, Chertow G (2017) Estimating the risk of radiocontrast-associated nephropathy. J Am Soc Nephrol 28(2):653–659. https://doi.org/10.1681/asn.2016010021
4. Nagle SK, Schiebler ML, Repplinger MD, Francois CJ, Vigen KK, Yarlagadda R, Grist TM, Reeder SB (2016) Contrast enhanced pulmonary magnetic resonance angiography for pulmonary embolism: building a successful program. Eur J Radiol 85(3):553–563. https://doi.org/10.1016/j.ejrad.2015.12.018

5. Russo RJ, Costa HS, Silva PD, Anderson JL, Arshad A, Biederman RW, Boyle NG, Frabizzio JV, Birgersdotter-Green U, Higgins SL, Lampert R, Machado CE, Martin ET, Rivard AL, Rubenstein JC, Schaerf RH, Schwartz JD, Shah DJ, Tomassoni GF, Tominaga GT, Tonkin AE, Uretsky S, Wolff SD (2017) Assessing the risks associated with mri in patients with a pacemaker or defibrillator. N Engl J Med 376(8):755–764. https://doi.org/10.1056/NEJMoa1603265
6. McDonald RJ, McDonald JS, Kallmes DF, Jentoft ME, Murray DL, Thielen KR, Williamson EE, Eckel LJ (2015) Intracranial gadolinium deposition after contrast-enhanced MR imaging. Radiology 275(3):772–782. https://doi.org/10.1148/radiol.15150025
7. Johns CS, Swift AJ, Hughes PJC, Ohno Y, Schiebler M, Wild JM (2017) Pulmonary MR angiography and perfusion imaging—a review of methods and applications. Eur J Radiol 86:361–370. https://doi.org/10.1016/j.ejrad.2016.10.003
8. Wild JM, Marshall H, Bock M, Schad LR, Jakob PM, Puderbach M, Molinari F, Van Beek EJ, Biederer J (2012) MRI of the lung (1/3): methods. Insights Imaging 3(4):345–353. https://doi.org/10.1007/s13244-012-0176-x
9. Hadizadeh DR, Marx C, Gieseke J, Schild HH, Willinek WA (2014) High temporal and high spatial resolution MR angiography (4D-MRA). RoFo Fortschr auf dem Geb der Rontgenstrahlen und der Nukl 186(9):847–859. https://doi.org/10.1055/s-0034-1366661
10. Korosec FR, Frayne R, Grist TM, Mistretta CA (1996) Time-resolved contrast-enhanced 3D MR angiography. Magn Reson Med 36(3):345–351
11. Vigen KK, Peters DC, Grist TM, Block WF, Mistretta CA (2000) Undersampled projection-reconstruction imaging for time-resolved contrast-enhanced imaging. Magn Reson Med 43(2):170–176
12. Du YP, Parker DL, Davis WL, Cao G (1994) Reduction of partial-volume artifacts with zero-filled interpolation in three-dimensional MR angiography. J Magn Reson Imaging 4(5):733–741
13. Du J, Bydder M (2007) High-resolution time-resolved contrast-enhanced MR abdominal and pulmonary angiography using a spiral-TRICKS sequence. Magn Reson Med 58(3):631–635. https://doi.org/10.1002/mrm.21298
14. Budjan J, Attenberger UI, Schoenberg SO, Pietsch H, Jost G (2018) The impact of injector-based contrast agent administration in time-resolved MRA. Eur Radiol 28(5):2246–2253. https://doi.org/10.1007/s00330-017-5178-0
15. Vasanawala SS, Nguyen K-L, Hope MD, Bridges MD, Hope TA, Reeder SB, Bashir MR (2016) Safety and technique offerumoxytol administration for MRI. Magn reson medicine 75(5):2107–2111. https://doi.org/10.1002/mrm.26151
16. Thakor AS, Chung J, Patel P, Chan A, Ahmed A, McNeil G, Liu DM, Forster B, Klass D (2017) Use of blood pool agents with steady-state MRI to assess the vascular system. J Magn Reson Imaging 45(6):1559–1572. https://doi.org/10.1002/jmri.25636
17. Bannas P, Bell LC, Johnson KM, Schiebler ML, Francois CJ, Motosugi U, Consigny D, Reeder SB, Nagle SK (2016) Pulmonary embolism detection with three-dimensional ultrashort echo time MR imaging: experimental study in Canines. Radiology 278(2):413–421. https://doi.org/10.1148/radiol.2015150606
18. Hui BK, Noga ML, Gan KD, Wilman AH (2005) Navigator-gated three-dimensional MR angiography of the pulmonary arteries using steady-state free precession. J Magn Reson Imaging 21(6):831–835. https://doi.org/10.1002/jmri.20334
19. Bitar R, Leung G, Perng R, Tadros S, Moody AR, Sarrazin J, McGregor C, Christakis M, Symons S, Nelson A, Roberts TP (2006) MR pulse sequences: what every radiologist wants to know but is afraid to ask. Radiographics 26(2):513–537. https://doi.org/10.1148/rg.262055063
20. Miyazaki M, Lee VS (2008) Nonenhanced MR angiography. Radiology 248(1):20–43. https://doi.org/10.1148/radiol.2481071497
21. Ley S, Ley-Zaporozhan J (2012) Pulmonary perfusion imaging using MRI: clinical application. Insights Imaging 3(1):61–71. https://doi.org/10.1007/s13244-011-0140-1
22. Suga K, Ogasawara N, Okada M, Tsukuda T, Matsunaga N, Miyazaki M (2002) Lung perfusion impairments in pulmonary embolic and airway obstruction with noncontrast MR imaging. J Appl Physiol 92(6):2439–2451. https://doi.org/10.1152/japplphysiol.00900.2001
23. Mai VM, Berr SS (1999) MR perfusion imaging of pulmonary parenchyma using pulsed arterial spin labeling techniques: FAIRER and FAIR. J Magn Reson Imaging 9(3):483–487
24. Greer JS, Maroules CD, Oz OK, Abbara S, Peshock RM, Pedrosa I, Madhuranthakam AJ (2018) Non-contrast quantitative pulmonary perfusion using flow alternating inversion recovery at 3T: a preliminary study. Magn Reson Imaging 46:106–113. https://doi.org/10.1016/j.mri.2017.11.007
25. Fischer A, Pracht ED, Arnold JF, Kotas M, Flentje M, Jakob PM (2008) Assessment of pulmonary perfusion in a single shot using SEEPAGE. J Magn Reson Imaging 27(1):63–70. https://doi.org/10.1002/jmri.21235
26. Messroghli DR, Moon JC, Ferreira VM, Grosse-Wortmann L, He T, Kellman P, Mascherbauer J, Nezafat R, Salerno M, Schelbert EB, Taylor AJ, Thompson R, Ugander M, van Heeswijk RB, Friedrich MG (2017) Clinical recommendations for cardiovascular magnetic resonance mapping of T1, T2, T2* and extracellular volume: a consensus statement by the society for cardiovascular magnetic resonance (SCMR) endorsed by the European association for cardiovascular imaging (EACVI). J Cardiovasc Magn Reson Off J Soc Cardiovasc Magn Reson 19(1):75. https://doi.org/10.1186/s12968-017-0389-8
27. Stein PD, Fowler SE, Goodman LR, Gottschalk A, Hales CA, Hull RD, Leeper KV Jr, Popovich J Jr, Quinn DA, Sos TA, Sostman HD, Tapson VF, Wakefield TW, Weg JG, Woodard PK (2006) Multidetector computed tomography for acute pulmonary embolism. N Engl J Med 354(22):2317–2327. https://doi.org/10.1056/NEJMoa052367
28. Pena E, Kimpton M, Dennie C, Peterson R, Le Gal G, Carrier M (2012) Difference in interpretation of computed tomography pulmonary angiography diagnosis of subsegmental thrombosis in patients with suspected pulmonary embolism. J Thromb Haemost 10(3):496–498. https://doi.org/10.1111/j.1538-7836.2011.04612.x
29. Benson DG, Schiebler ML, Repplinger MD, Francois CJ, Grist TM, Reeder SB, Nagle SK (2017) Contrast-enhanced pulmonary MRA for the primary diagnosis of pulmonary embolism: current state of the art and future directions. Br J Radiol 90(1074):20160901. https://doi.org/10.1259/bjr.20160901
30. Amundsen T, Torheim G, Kvistad KA, Waage A, Bjermer L, Nordlid KK, Johnsen H, Asberg A, Haraldseth O (2002) Perfusion abnormalities in pulmonary embolism studied with perfusion MRI and ventilation-perfusion scintigraphy: an intra-modality and inter-modality agreement study. J Magn Reson Imaging 15(4):386–394
31. Johns CS, Swift AJ, Rajaram S, Hughes PJC, Capener DJ, Kiely DG, Wild JM (2017) Lung perfusion: MRI vs. SPECT for screening in suspected chronic thromboembolic pulmonary hypertension. J Magn reson imaging : JMRI 46 (6):1693–1697. https://doi.org/10.1002/jmri.25714
32. Stein PD, Chenevert TL, Fowler SE, Goodman LR, Gottschalk A, Hales CA, Hull RD, Jablonski KA, Leeper KV Jr, Naidich DP, Sak DJ, Sostman HD, Tapson VF, Weg JG, Woodard PK (2010) Gadolinium-enhanced magnetic resonance angiography for pulmonary embolism: a multicenter prospective study (PIOPED III).

Ann Intern Med 152(7):434–443. https://doi.org/10.7326/0003-4819-152-7-201004060-00008
33. Revel MP, Sanchez O, Couchon S, Planquette B, Hernigou A, Niarra R, Meyer G, Chatellier G (2012) Diagnostic accuracy of magnetic resonance imaging for an acute pulmonary embolism: results of the 'IRM-EP' study. J Thromb Haemost 10(5):743–750. https://doi.org/10.1111/j.1538-7836.2012.04652.x
34. Schiebler ML, Nagle SK, Francois CJ, Repplinger MD, Hamedani AG, Vigen KK, Yarlagadda R, Grist TM, Reeder SB (2013) Effectiveness of MR angiography for the primary diagnosis of acute pulmonary embolism: clinical outcomes at 3 months and 1 year. J Magn Reson Imaging 38(4):914–925. https://doi.org/10.1002/jmri.24057
35. Kalb B, Sharma P, Tigges S, Ray GL, Kitajima HD, Costello JR, Chen Z, Martin DR (2012) MR imaging of pulmonary embolism: diagnostic accuracy of contrast-enhanced 3D MR pulmonary angiography, contrast-enhanced low-flip angle 3D GRE, and non-enhanced free-induction FISP sequences. Radiology 263(1):271–278. https://doi.org/10.1148/radiol.12110224
36. Bannas P, Schiebler ML, Motosugi U, Francois CJ, Reeder SB, Nagle SK (2014) Pulmonary MRA: differentiation of pulmonary embolism from truncation artefact. Eur Radiol 24(8):1942–1949. https://doi.org/10.1007/s00330-014-3219-5
37. Kluge A, Muller C, Hansel J, Gerriets T, Bachmann G (2004) Real-time MR with TrueFISP for the detection of acute pulmonary embolism: initial clinical experience. Eur Radiol 14(4):709–718. https://doi.org/10.1007/s00330-003-2164-5
38. Ohno Y, Koyama H, Matsumoto K, Onishi Y, Nogami M, Takenaka D, Yoshikawa T, Matsumoto S, Sugimura K (2010) Dynamic MR perfusion imaging: capability for quantitative assessment of disease extent and prediction of outcome for patients with acute pulmonary thromboembolism. J Magn Reson Imaging 31(5):1081–1090. https://doi.org/10.1002/jmri.22146
39. Wirth G, Bruggemann K, Bostel T, Mayer E, Duber C, Kreitner KF (2014) Chronic thromboembolic pulmonary hypertension (CTEPH)-potential role of multidetector-row CT (MD-CT) and MR imaging in the diagnosis and differential diagnosis of the disease. RoFo Fortschr auf dem Geb der Rontgenstrahlen und der Nukl 186(8):751–761. https://doi.org/10.1055/s-0034-1366425
40. Ley S, Kauczor HU, Heussel CP, Kramm T, Mayer E, Thelen M, Kreitner KF (2003) Value of contrast-enhanced MR angiography and helical CT angiography in chronic thromboembolic pulmonary hypertension. Eur Radiol 13(10):2365–2371. https://doi.org/10.1007/s00330-003-1878-8
41. Ley S, Ley-Zaporozhan J, Pitton MB, Schneider J, Wirth GM, Mayer E, Duber C, Kreitner KF (2012) Diagnostic performance of state-of-the-art imaging techniques for morphological assessment of vascular abnormalities in patients with chronic thromboembolic pulmonary hypertension (CTEPH). Eur Radiol 22(3):607–616. https://doi.org/10.1007/s00330-011-2290-4
42. Kreitner KF, Kunz RP, Ley S, Oberholzer K, Neeb D, Gast KK, Heussel CP, Eberle B, Mayer E, Kauczor HU, Duber C (2007) Chronic thromboembolic pulmonary hypertension - assessment by magnetic resonance imaging. Eur Radiol 17(1):11–21. https://doi.org/10.1007/s00330-006-0327-x
43. Rajaram S, Swift AJ, Capener D, Telfer A, Davies C, Hill C, Condliffe R, Elliot C, Hurdman J, Kiely DG, Wild JM (2012) Diagnostic accuracy of contrast-enhanced MR angiography and unenhanced proton MR imaging compared with CT pulmonary angiography in chronic thromboembolic pulmonary hypertension. Eur Radiol 22(2):310–317. https://doi.org/10.1007/s00330-011-2252-x
44. Rajaram S, Swift AJ, Telfer A, Hurdman J, Marshall H, Lorenz E, Capener D, Davies C, Hill C, Elliot C, Condliffe R, Wild JM, Kiely DG (2013) 3D contrast-enhanced lung perfusion MRI is an effective screening tool for chronic thromboembolic pulmonary hypertension: results from the ASPIRE registry. Thorax 68(7):677–678. https://doi.org/10.1136/thoraxjnl-2012-203020
45. Ley S, Fink C, Zaporozhan J, Borst MM, Meyer FJ, Puderbach M, Eichinger M, Plathow C, Grunig E, Kreitner KF, Kauczor HU (2005) Value of high spatial and high temporal resolution magnetic resonance angiography for differentiation between idiopathic and thromboembolic pulmonary hypertension: initial results. Eur Radiol 15(11):2256–2263. https://doi.org/10.1007/s00330-005-2792-z
46. Schoenfeld C, Cebotari S, Hinrichs J, Renne J, Kaireit T, Olsson KM, Voskrebenzev A, Gutberlet M, Hoeper MM, Welte T, Haverich A, Wacker F, Vogel-Claussen J (2016) MR imaging-derived regional pulmonary parenchymal perfusion and cardiac function for monitoring patients with chronic thromboembolic pulmonary hypertension before and after pulmonary endarterectomy. Radiology 279(3):925–934. https://doi.org/10.1148/radiol.2015150765
47. Swift AJ, Rajaram S, Marshall H, Condliffe R, Capener D, Hill C, Davies C, Hurdman J, Elliot CA, Wild JM, Kiely DG (2012) Black blood MRI has diagnostic and prognostic value in the assessment of patients with pulmonary hypertension. Eur Radiol 22(3):695–702. https://doi.org/10.1007/s00330-011-2306-0
48. Frank H, Globits S, Glogar D, Neuhold A, Kneussl M, Mlczoch J (1993) Detection and quantification of pulmonary artery hypertension with MR imaging: results in 23 patients. AJR Am J Roentgenol 161(1):27–31. https://doi.org/10.2214/ajr.161.1.8517315
49. Sanz J, Kuschnir P, Rius T, Salguero R, Sulica R, Einstein AJ, Dellegrottaglie S, Fuster V, Rajagopalan S, Poon M (2007) Pulmonary arterial hypertension: noninvasive detection with phase-contrast MR imaging. Radiology 243(1):70–79. https://doi.org/10.1148/radiol.2431060477
50. Ley S, Mereles D, Risse F, Grunig E, Ley-Zaporozhan J, Tecer Z, Puderbach M, Fink C, Kauczor HU (2007) Quantitative 3D pulmonary MR-perfusion in patients with pulmonary arterial hypertension: correlation with invasive pressure measurements. Eur J Radiol 61(2):251–255. https://doi.org/10.1016/j.ejrad.2006.08.028
51. Ohno Y, Hatabu H, Murase K, Higashino T, Nogami M, Yoshikawa T, Sugimura K (2007) Primary pulmonary hypertension: 3D dynamic perfusion MRI for quantitative analysis of regional pulmonary perfusion. AJR Am J Roentgenol 188(1):48–56. https://doi.org/10.2214/ajr.05.0135
52. Skrok J, Shehata ML, Mathai S, Girgis RE, Zaiman A, Mudd JO, Boyce D, Lechtzin N, Lima JA, Bluemke DA, Hassoun PM, Vogel-Claussen J (2012) Pulmonary arterial hypertension: MR imaging-derived first-pass bolus kinetic parameters are biomarkers for pulmonary hemodynamics, cardiac function, and ventricular remodeling. Radiology 263(3):678–687. https://doi.org/10.1148/radiol.12111001
53. Swift AJ, Telfer A, Rajaram S, Condliffe R, Marshall H, Capener D, Hurdman J, Elliot C, Kiely DG, Wild JM (2014) Dynamic contrast-enhanced magnetic resonance imaging in patients with pulmonary arterial hypertension. Pulm Circ 4(1):61–70. https://doi.org/10.1086/674882
54. Reiter G, Reiter U, Kovacs G, Olschewski H, Fuchsjager M (2015) Blood flow vortices along the main pulmonary artery measured with MR imaging for diagnosis of pulmonary hypertension. Radiology 275(1):71–79. https://doi.org/10.1148/radiol.14140849
55. Ley S, Fink C, Risse F, Ehlken N, Fischer C, Ley-Zaporozhan J, Kauczor HU, Klose H, Gruenig E (2013) Magnetic resonance imaging to assess the effect of exercise training on pulmonary perfusion and blood flow in patients with pulmonary hypertension. Eur Radiol 23(2):324–331. https://doi.org/10.1007/s00330-012-2606-z
56. Goerne H, Chaturvedi A, Partovi S, Rajiah P (2018) State-of-the-art pulmonary arterial imaging—Part 2. VASA Z fur

Gefasskrankheiten 47(5):361–375. https://doi.org/10.1024/0301-1526/a000709
57. Mohrs OK, Voigtlander T, Heussel CP, Bardeleben S, Duber C, Kreitner KF (2002) Morphologic and functional assessment of vascular abnormalities of the pulmonary vasculature by breath-hold MR techniques. RoFo Fortschr auf dem Geb der Rontgenstrahlen und der Nukl 174(4):467–473. https://doi.org/10.1055/s-2002-25115
58. Maki DD, Siegelman ES, Roberts DA, Baum RA, Gefter WB (2001) Pulmonary arteriovenous malformations: three-dimensional gadolinium-enhanced MR angiography-initial experience. Radiology 219(1):243–246. https://doi.org/10.1148/radiology.219.1.r01ap50243
59. Shimohira M, Kawai T, Hashizume T, Ohta K, Nakagawa M, Ozawa Y, Sakurai K, Shibamoto Y (2015) Reperfusion rates of pulmonary arteriovenous malformations after coil embolization: evaluation with time-resolved MR angiography or pulmonary angiography. J Vasc Interv Radiol 26(6):856–864.e851. https://doi.org/10.1016/j.jvir.2015.02.016
60. Wielputz MO, Puderbach M, Kopp-Schneider A, Stahl M, Fritzsching E, Sommerburg O, Ley S, Sumkauskaite M, Biederer J, Kauczor HU, Eichinger M, Mall MA (2014) Magnetic resonance imaging detects changes in structure and perfusion, and response to therapy in early cystic fibrosis lung disease. Am J Respir Crit Care Med 189(8):956–965. https://doi.org/10.1164/rccm.201309-1659OC
61. Bauman G, Puderbach M, Heimann T, Kopp-Schneider A, Fritzsching E, Mall MA, Eichinger M (2013) Validation of Fourier decomposition MRI with dynamic contrast-enhanced MRI using visual and automated scoring of pulmonary perfusion in young cystic fibrosis patients. Eur J Radiol 82(12):2371–2377. https://doi.org/10.1016/j.ejrad.2013.08.018
62. Fan L, Xia Y, Guan Y, Yu H, Zhang TF, Liu SY, Li B (2013) Capability of differentiating smokers with normal pulmonary function from COPD patients: a comparison of CT pulmonary volume analysis and MR perfusion imaging. Eur Radiol 23(5):1234–1241. https://doi.org/10.1007/s00330-012-2729-2
63. Ohno Y, Hatabu H, Murase K, Higashino T, Kawamitsu H, Watanabe H, Takenaka D, Fujii M, Sugimura K (2004) Quantitative assessment of regional pulmonary perfusion in the entire lung using three-dimensional ultrafast dynamic contrast-enhanced magnetic resonance imaging: preliminary experience in 40 subjects. J Magn Reson Imaging 20(3):353–365. https://doi.org/10.1002/jmri.20137
64. Jang YM, Oh YM, Seo JB, Kim N, Chae EJ, Lee YK, Lee SD (2008) Quantitatively assessed dynamic contrast-enhanced magnetic resonance imaging in patients with chronic obstructive pulmonary disease: correlation of perfusion parameters with pulmonary function test and quantitative computed tomography. Invest Radiol 43(6):403–410. https://doi.org/10.1097/RLI.0b013e31816901ab
65. Ley-Zaporozhan J, Ley S, Kauczor HU (2008) Morphological and functional imaging in COPD with CT and MRI: present and future. Eur Radiol 18(3):510–521. https://doi.org/10.1007/s00330-007-0772-1
66. Sergiacomi G, Taglieri A, Chiaravalloti A, Calabria E, Arduini S, Tosti D, Citraro D, Pezzuto G, Puxeddu E, Simonetti G (2014) Acute COPD exacerbation: 3 T MRI evaluation of pulmonary regional perfusion–preliminary experience. Respir Med 108(6):875–882. https://doi.org/10.1016/j.rmed.2014.04.002
67. Xia Y, Guan Y, Fan L, Liu SY, Yu H, Zhao LM, Li B (2014) Dynamic contrast enhanced magnetic resonance perfusion imaging in high-risk smokers and smoking-related COPD: correlations with pulmonary function tests and quantitative computed tomography. COPD 11(5):510–520. https://doi.org/10.3109/15412555.2014.948990
68. Fan L, Xia Y, Guan Y, Zhang TF, Liu SY (2014) Characteristic features of pulmonary function test, CT volume analysis and MR perfusion imaging in COPD patients with different HRCT phenotypes. Clin Respir J 8(1):45–54. https://doi.org/10.1111/crj.12033
69. Yi CA, Lee KS, Han J, Chung MP, Chung MJ, Shin KM (2008) 3-T MRI for differentiating inflammation- and fibrosis-predominant lesions of usual and nonspecific interstitial pneumonia: comparison study with pathologic correlation. AJR Am J Roentgenol 190(4):878–885. https://doi.org/10.2214/ajr.07.2833
70. Ohno Y, Nishio M, Koyama H, Seki S, Tsubakimoto M, Fujisawa Y, Yoshikawa T, Matsumoto S, Sugimura K (2015) Solitary pulmonary nodules: comparison of dynamic first-pass contrast-enhanced perfusion area-detector CT, dynamic first-pass contrast-enhanced MR imaging, and FDG PET/CT. Radiology 274(2):563–575. https://doi.org/10.1148/radiol.14132289
71. Ohno Y, Nishio M, Koyama H, Yoshikawa T, Matsumoto S, Seki S, Sugimura K (2014) Journal club: comparison of assessment of preoperative pulmonary vasculature in patients with non-small cell lung cancer by non-contrast- and 4D contrast-enhanced 3-T MR angiography and contrast-enhanced 64-MDCT. AJR Am J Roentgenol 202(3):493–506. https://doi.org/10.2214/ajr.13.10833
72. Ohno Y, Seki S, Koyama H, Yoshikawa T, Matsumoto S, Takenaka D, Kassai Y, Yui M, Sugimura K (2015) 3D ECG- and respiratory-gated non-contrast-enhanced (CE) perfusion MRI for postoperative lung function prediction in non-small-cell lung cancer patients: a comparison with thin-section quantitative computed tomography, dynamic CE-perfusion MRI, and perfusion scan. J Magn Reson Imaging 42(2):340–353. https://doi.org/10.1002/jmri.24800
73. Oldan JD, Klem I, Borges-Neto S (2014) Pulmonary venous stenosis on ventilation-perfusion scintigraphy: a correlation with dynamic magnetic resonance pulmonary angiography. Clin Nucl Med 39(3):292–294. https://doi.org/10.1097/rlu.0000000000000344